# Strain-level differences in gut microbiome composition determine fecal IgA levels and are modifiable by gut microbiota manipulation

*Chao Yang,[1,2] Ilaria Mogno,[1,2] Eduardo J. Contijoch,[1,2] Joshua N. Borgerding,[1] Varun Aggarwala,[1,2] Zhihua Li,[2] Emilie K. Grasset*,[1,6] *Drew S. Helmus[3], Marla C. Dubinsky[3], Saurabh Mehandru,[1] Andrea Cerutti,[1,4,5] and Jeremiah J. Faith[1,2,*]*

[1]Precision Immunology Institute, Icahn School of Medicine at Mount Sinai, New York, NY 10029, USA

[2]Institute for Genomics and Multiscale Biology, Icahn School of Medicine at Mount Sinai, New York, NY 10029, USA

[3]Pediatric Gastroenterology and Hepatology, Department of Pediatrics, Susan and Leonard Feinstein IBD Clinical Center, Icahn School of Medicine at Mount Sinai, New York, NY 10029, USA

[4]Program for Inflammatory and Cardiovascular Disorders, Institut Hospital del Mar d'Investigacions Mediques (IMIM), Barcelona 08003, Spain

[5]Catalan Institute for Advanced Studies (ICREA), Barcelona 08003, Spain

[6]Department of Medicine, Center for Molecular Medicine, Karolinska Institutet, Karolinska University Hospital, SE-171 77 Stockholm, Sweden

*Correspondence: jeremiah.faith@mssm.edu (J.J.F.)

## Keywords

Gut microbiota, Immunoglobulin A, *Bacteroides ovatus*, Fecal Microbiota Transplantation, Immune modulation

## Abstract

Fecal IgA production depends on colonization by a gut microbiota. However, the bacterial strains that drive gut IgA production remain largely unknown. By accessing the IgA-inducing capacity of a diverse set of human gut microbial strains, we identified *Bacteroides ovatus* as the species that best induced gut IgA production. However, this induction varied biomodally across different *B. ovatus* strains. The high IgA-inducing *B. ovatus* strains preferentially elicited more IgA production in the large intestine through both T-cell-dependent and T-cell-independent B cell-activation pathways. Remarkably, a low-IgA phenotype in mice could be robustly and consistently converted into a high-IgA phenotype by transplanting a multiplex cocktail of high IgA-inducing *B. ovatus* strains but not individual ones. Thus, microbial strain specificity is essential for the optimal induction of high-IgA responses in the gut. Our results highlight the critical importance of microbial strains in driving phenotype variation in the mucosal immune system and provide a strategy to robustly modify a gut immune phenotype, including IgA production.

## Introduction

Immunoglobulin A (IgA) is the most abundant mucosal antibody and plays an essential role in maintaining gut homeostasis as well as other physiological processes[1-3]. Secretory IgA, for example, can limit the access of bacteria and bacteria-derived toxins to intestinal epithelial cells[4,5], facilitate the clearance of bacteria that have breached the mucosal barrier[6-8] and regulate the colonization of bacteria in the mucosal lining[9,10]. In addition, IgA can also bind disease-associated gut microbiota[11-13]. Conversely, the gut microbiota and its metabolites drive the production of IgA as germ-free (GF) mice have an almost undetectable level of fecal IgA[14]. Upon bacteria colonization, even with a single bacterial strain[15-17], B cells undergo class-switch to $IgA^+$ cells in gut-associated lymphoid tissues (GALT), which include Peyer's patches (PP), isolated lymphoid follicles (ILF) and mesenteric lymph nodes (MLN), and in the gut lamina propria (LP)[8,18]. Much of the intestinal IgA is bacteria-specific[15,16,19], and the B-cell repertoire is highly influenced by the microbiota composition[20]. To date, a few murine derived bacterial species have been identified as being able to enhance or reduce intestinal IgA production[21-25]. However, key questions regarding the impact of microbiota in this process remain largely unanswered including the importance of colonization order, the contribution of individual bacterial species versus that of microbial communities, the potential to modulate IgA production by altering gut microbiota composition with commensal organisms, and the role of each microbial species in the development of $IgA^+$ B cells in specific tissues[8,26].

Apart from IgA-secreting cells, the gut microbiota has the capacity to influence numerous other immune cell populations including colonic regulatory T cells[27-29], IL-17 producing T helper cells[30], and macrophages[31]. Importantly, many of these responses seem to be bacterial strain-specific as communities with comparable species composition can drive gut immune responses characterized by largely different cell compositions[32]. These discoveries indicate that manipulation of the gut microbiota, with appropriate bacterial strains, represents a potential therapeutic pathway for the treatment of diseases including inflammatory bowel disease,

68 rheumatoid arthritis and multiple sclerosis through shaping the host immune system[33]. Although
69 the studies of microbiota-based therapeutics (MT) and fecal microbiota transplantation (FMT)
70 have heavily focused on the engraftment of the transmitted microbiota and its influence on the
71 composition of the recipient microbiota[34-37], the clinical application of microbiota manipulation as
72 an immunomodulatory strategy will require combinations of bacterial strains optimized for the
73 induction of specific immune phenotypes that are robust to the interpersonal variation in the pre-
74 existing microbiota of each recipient.

75 Here we demonstrate that, upon transfer into GF mice, human isolates of the *Bacteroides*
76 *ovatus* species, one of the most common human gut commensals, are uniquely capable of
77 inducing high mucosal IgA production compared with other common gut commensal species.
78 This IgA-inducing capacity, however, was restricted to specific strains of *B. ovatus* that
79 preferentially led to IgA production in the large intestine through both T-cell-dependent (TD) and
80 T-cell-independent (TI) B cell-activation pathways. While no individual bacterial strain functioned
81 as an effective enhancer of gut IgA production, we found that cocktails of these high IgA-
82 inducing ($IgA^{high}$) strains could serve as effective immunomodulators, that elicited higher fecal
83 IgA levels upon administration to animals harboring a pre-existing microbiota with low IgA-
84 inducing potential ($IgA^{low}$). Our work demonstrates the importance of strain-level variation in gut
85 microbiota composition on mucosal immune responses. It also supports the potential utility of
86 cultured multi-bacterial effector strain cocktails as a strategy to overcome phenotype transfer
87 resistance in microbiota-based immunomodulation[38].
88

## Results

### *B. ovatus* elicits robust gut IgA production

To determine if individual gut bacterial species have a distinct IgA-inducing potential, we monocolonized GF C57BL/6 mice with one of eight different human gut commensal bacteria (Supplementary Table 1) with representatives from the most prominent phyla of the human gut including Firmicutes, Bacteroidetes, Actinobacteria and Proteobacteria[39,40]. After three weeks of colonization to allow optimal steady-state gut IgA secretion (Supplementary Fig. 1a), we measured serum and fecal IgA levels in each group of gnotobiotic mice[16]. Although all tested species significantly increased IgA level relative to control GF mice, *B. ovatus* monocolonized mice secreted significantly more IgA in their feces compared with mice colonized with any of the other seven human gut bacteria (Fig. 1a; $p < 0.001$). Most species also increased serum IgA (Supplementary Fig. 1b). However, consistent with previous reports[18], fecal IgA and serum IgA levels in these mice did not correlate significantly (Supplementary Fig. 1c; $R^2 = 0.226$; $p = 0.196$). GF mice colonized with the cocktail of all eight bacterial species yielded as much fecal and serum IgA as mice monocolonized with *B. ovatus*.

To address if the order of bacterial colonization could influence fecal IgA secretion, GF mice were sequentially colonized every three weeks with individual species or small cocktails of the same eight bacterial species. We first assayed fecal IgA level in mice sequentially colonized with low IgA inducers (e.g. *E. coli*) to high IgA inducers (e.g. *B. ovatus*). Fecal IgA increased gradually with the colonization of additional bacterial species. However, the more striking (>2-fold) increase in IgA occurred after colonization with *B. ovatus* (Fig. 1b). Metagenomic sequencing of fecal microbiota in these mice revealed gut colonization by each bacterial species, albeit with different proportions (Fig. 1c). We then reversed the order of colonization from high IgA inducers (e.g. *B. ovatus*) to low IgA inducers (Fig. 1d). Once again, *B. ovatus* elicited the largest increase of fecal IgA production, while the other species led to smaller increases (Fig. 1e). Remarkably, the relative abundance of each organism at the end of the

115 colonization was very similar, regardless of the order of colonization (Fig. 1c,e). These results
116 demonstrate that *B. ovatus* is a uniquely potent gut IgA inducer and that the species
117 composition of the gut microbiota impacts IgA production more than the order of bacterial
118 colonization.

119 To test the role of bacterial viability in the induction of gut IgA by *B. ovatus*[15,41,42], GF mice
120 were administered heat-killed *B. ovatus* or *B. ovatus* metabolites (i.e. filtered growth medium
121 from stationary phase of *B. ovatus* cultures) for three weeks. Neither approach was capable of
122 enhancing fecal IgA above the level detected in GF mice (Supplementary Fig. 1d). To ensure
123 the above result was not due to the underdeveloped mucosal immune system of GF mice, we
124 performed similar experiments by first colonizing GF mice with *E. coli* for three weeks and
125 subsequently treated these mice with heat-killed *B. ovatus* for an additional three weeks. Again,
126 we found no significant fecal IgA increase (Supplementary Fig. 1d). Thus, neither dead *B.*
127 *ovatus* nor its metabolites triggered efficient gut IgA responses in the murine intestine. All
128 together, live *B. ovatus* species elicited more gut IgA production than other tested gut
129 commensal bacterial species in GF mice.
130
131 **_B. ovatus_-driven gut IgA production is strain-specific**
132 Given the remarkable microbial strain variation across individuals[43-46], we wondered whether all
133 *B. ovatus* strains within this common bacterial species induced comparably high fecal IgA. GF
134 mice monocolonized for three weeks with one of 19 *B. ovatus* strains isolated from 19 different
135 individuals (Supplementary Table 2) showed a strain-specific gut IgA response (Fig. 1f; $p <$
136 0.0001 one-way ANOVA). In contrast to the large variability of fecal IgA levels, serum IgA levels
137 were comparable across mice monocolonized with different *B. ovatus* strains (Supplementary
138 Fig. 1e). Similarly, the colonization density was also comparable across mice harboring different
139 *B. ovatus* strains (Supplementary Fig. 1f). This observation suggests that the global density of
140 each individual strain was not implicated in the genesis of strain-specific differences of gut IgA

responses. Of note, the distribution pattern of IgA induction across multiple *B. ovatus* strains was bimodal (Supplementary Fig. 1g; $p$ = 0.0481 Hartigans' Dip Test), allowing these strains to be categorized as $IgA^{high}$ or $IgA^{low}$. The genomic similarity of *B. ovatus* strains was not a significant predictor of their $IgA^{high}$ and $IgA^{low}$ properties (Fig. 1g and Supplementary Table 3), which suggests that their distinct IgA-inducing function is shared amongst the species rather than representing an evolutionarily distinct group within the species.

To rule out a bias in our preliminary screen for $IgA^{low}$ strains within the *Bacteroides* genus, we assayed whether additional strains could induce high fecal IgA (Fig. 1a). We found no strain-specific differences in fecal IgA induction when GF mice were monocolonized with three distinct strains of *B. caccae*, *B. thetaiotaomicron* and *B. vulgatus* (Supplementary Fig. 1h). The IgA-inducing function of additional common species from the order Bacteroidales, including *Parabacteroides johnsonii*, *Bacteroides intestinalis* and *Bacteroides fragilis,* were tested but also induced much less gut IgA than *B. ovatus* (Supplementary Fig. 1h). These results indicate that the high IgA-inducing ability of *B. ovatus* is unique to this gut bacterial species and only to a subset of strains.

To examine the influence of *B. ovatus* strain variation on host fecal IgA production in the context of more complex gut microbiotas, we colonized GF mice with one of the seven microbiota arrayed culture collections originally isolated from different human donors with each collection consisting of 15-20 unique species[32]. The arrayed culture collections were assembled to reconstitute a donor microbiota each containing a unique *B. ovatus* strain, which was already functionally tested by earlier monocolonization (Fig. 1f). We observed a significant positive correlation between the fecal IgA concentrations induced by an individual *B. ovatus* strain and the fecal IgA concentrations elicited by a culture collection representing the entire *B. ovatus*-containing microbiota from the same donor (Fig. 1h; $R^2$ = 0.859, $p$ = 0.0027). Again, these results suggest that the *B. ovatus* strain composition is a major contributor of gut IgA responses even when considered in the context of complex microbial communities.

Unlike inbred laboratory mice housed in a highly controlled environment, human beings, with different genetic background, are exposed to more complex continuum of factors including some that were demonstrated to affect fecal IgA production such as genetics and diet[47,48]. To determine whether *B. ovatus* could drive robust gut IgA responses also in humans, we measured the fecal concentration of IgA in multiple human donors and correlated this concentration with that of fecal IgA generated by GF mice monocolonized with a *B. ovatus* strain isolated from identical donors. Though no significant correlation was observed, there was a clear trend towards a positive correlation even in an uncontrolled condition (Fig. 1i; $R^2 = 0.2071$, $p = 0.0765$).

In total these results demonstrate that a subset of *B. ovatus* strains induce high fecal IgA levels, which broadly influence the total fecal IgA output of the host even in the context of a diverse gut microbiota.

**IgA$^{high}$ *B. ovatus* strains induce more IgA production in the large intestine**

To interrogate the mechanisms underpinning gut IgA induction by different *B. ovatus* strains, GF mice were colonized with a representative IgA$^{high}$ or IgA$^{low}$ strain (*B. ovatus* strain *E* and *Q,* respectively). We quantified bacteria-bound IgA in the stool of mice. Monocolonization with the IgA$^{high}$ strain *E* not only induced more free fecal IgA but also more fecal bacteria-bound IgA than the IgA$^{low}$ strain *Q* did (52.9% vs. 21.0% IgA-coated *B. ovatus*) (Fig. 2a). In contrast, no significant difference was observed in serum immunoglobulin isotypes (i.e. IgA, IgG1, IgG2a, IgG2b, IgG3, IgM and IgE) in monocolonized mice harboring either *B. ovatus* strain *E* or *Q* (Supplementary Fig. 1e, 2a).

Fecal IgA mostly derives from polymeric IgA released by IgA$^{+}$ plasma cells residing in the intestinal LP and translocated to the gut lumen across epithelial cells via transcytosis[49]. This process is mediated by a basolateral IgA (and IgM) transporter termed polymeric immunoglobulin receptor (pIgR)[49]. Independent groups have reported that the expression of

pIgR by gut epithelial cells is influenced by bacteria stimulation both *in vivo* and *in vitro*[50,51]. To determine if *B. ovatus* strain variation impacts fecal IgA level by modulating pIgR-mediated transcytosis, we imaged the expression of pIgR by immunofluorescence staining in the small intestine and the colon of mice colonized with either *B. ovatus* strain *E* ($IgA^{high}$) or *Q* ($IgA^{low}$). However, no noticeable difference in pIgR expression was observed (Supplementary Fig. 2b). To further interrogate the mechanism underpinning the increased fecal IgA in *B. ovatus* strain *E* colonized mice, we then quantified, by histology and flow cytometry, $IgA^+$ B cells in both small intestine and the colon. We found more $IgA^+$ B cells in the colonic LP of mice harboring *B. ovatus* strain *E* compared to mice harboring strain *Q*, while no significant strain-specific difference was observed in the small intestine (Fig. 2b,c). Although PPs and MLNs usually serve as dominant IgA inductive sites[52,53], we did not observe a significant difference in $IgA^+$ B cells at these sites by strain *E* or strain *Q* (Supplementary Fig. 3).

Given the preferential expansion of $IgA^+$ B cells in the colons of monocolonized mice harboring *B. ovatus* strain *E*, we then explored whether luminal IgA levels would vary between small and large intestinal regions. In the small intestine, we found that mice monocolonized with *B. ovatus* strain *E* or strain *Q* had comparable luminal IgA levels (Fig. 2d). In contrast, mice monocolonized with strain *E* had significantly more luminal IgA from cecum to distal colon than those colonized with strain *Q* (Fig. 2d). Similar results were also observed across all tested $IgA^{high}$ and $IgA^{low}$ *B. ovatus* strains (Supplementary Fig. 4). Thus, the $IgA^{high}$ *B. ovatus* strains induce more colonic IgA-secreting cells compared to $IgA^{low}$ *B. ovatus* strains, which results in the secretion of more IgA in the large intestinal lumen.

To determine if these observations were unique to GF C57BL/6 mice, we recapitulated our monocolonization strategy in GF Swiss Webster mice and found that fecal IgA was largely comparable in gnotobiotic C57BL/6 and Swiss Webster mice colonized with identical bacterial strains (Supplementary Fig. 5a-d; $R^2 = 0.601$, $p = 0.0011$). Moreover, $IgA^{high}$ strain colonized gnotobiotic Swiss Webster mice also secreted more intraluminal IgA in the large intestine

compared with IgA$^{low}$ strain colonized mice (Supplementary Fig. 5e). Thus, bacteria-induced gut IgA production is similar across different host genetic backgrounds.

**_B. ovatus_ elicits gut IgA production via both TD and TI B cell-activation pathways**

Gut IgA responses occur through TD or TI B cell-activation pathways[52,54]. To determine the influence of CD4$^+$ T cells on the gut IgA production induced by *B. ovatus*, we depleted CD4$^+$ T cells in mice by injecting with an anti-CD4 antibody five days prior to and for three weeks after monocolonization with *B. ovatus* strain *E* (Fig. 3a and Supplementary Fig. 6a-c). On day seven post-colonization, fecal IgA increased in both T cell-depleted and T cell-sufficient gnotobiotic mice, which suggests that CD4$^+$ T cells are not a dominant factor in early stage IgA induction. By day 14 post-colonization, control mice receiving an isotype-matched irrelevant antibody generated significantly more fecal IgA than mice receiving anti-CD4 antibody (Fig. 3b). In addition to reduced free IgA, *B. ovatus*-bound IgA also decreased in the stool of CD4$^+$ T cell-depleted mice (Fig. 3c). In both small intestine and the colon, the frequency of IgA$^+$ B cells was reduced by approximately 1/3 compared to that of IgA$^+$ B cells being detected in the control CD4$^+$ T cell-sufficient mice (Fig. 3d and Supplementary Fig. 6d,e). In addition, these control mice showed more intraluminal IgA than CD4$^+$ T cell-depleted mice across the whole intestinal tract (Fig. 3e).

**Multiplex cocktail of _B. ovatus_ strains robustly modify gut IgA production**

Given the potential of gut microbiota manipulation as a therapeutic, we next determined whether the high-IgA phenotype could be transferred to mice harboring microbiotas that induce a low level of fecal IgA. For this purpose, we recolonized GF C57BL/6 mice with either *B. ovatus* strain *E* (IgA$^{high}$) or *Q* (IgA$^{low}$) for three weeks, followed by cohousing these mice for an additional three weeks (Fig. 4a). After cohousing, mice monocolonized with *B. ovatus* strain *Q* showed no significant change in fecal IgA. In contrast, mice colonized initially with *B. ovatus*

strain *E* had reduced fecal IgA, which raised the possibility that the low-IgA phenotype behaves as a dominant character in the context of this simple bacterial community (Fig. 4b). Interestingly, the IgA$^{low}$ *B. ovatus* strain *Q* also dominated the relative abundance of the microbiota, as it represented ~95% of the microbiota compared with ~5% of *B. ovatus* strain *E* (Fig. 4c). In an attempt to overcome this resistance to transfer of the high-IgA phenotype to mice with low-IgA phenotype, we performed a similar experiment but added three more IgA$^{high}$ *B. ovatus* strains. Under these conditions, the high-IgA phenotype was transfered to the cohoused mice initially monocolonized with the IgA$^{low}$ strain (Supplementary Fig. 7a). However, *B. ovatus* strain *Q* still represented a substantial proportion (32.5 ~ 53.8%) of the relative abundance in this bacterial community (Supplementary Fig. 7b). Thus, a multiplex cocktail of bacterial effector strains that each individually can induce a specific phenotype provides a more robust strategy for transferring a high-IgA phenotype.

Beyond cohousing, we further validated the above findings by transferring IgA$^{high}$ strains therapeutically by oral gavage. Consistent with the cohousing results, mice first colonized with an IgA$^{low}$ *B. ovatus* strain and then orally gavaged with an additional IgA$^{high}$ strain did not alter gut IgA secretion. In contrast, mice receiving a cocktail of four IgA$^{high}$ *B. ovatus* strains (*B. ovatus* 4M) produced significantly more fecal IgA (Fig. 4d and Supplementary Table 4). Metagenomic sequencing results demonstrated that multiple *B. ovatus* strains colonized the recipient mice (Fig. 4e). Of note, IgA$^{low}$ *B. ovatus* strain *Q* still dominated the relative abundance of the gut microbiota in individual strain transfers (Fig. 4e). IgA$^{high}$ strains accounted for 44% of the gut microbiota in the *B. ovatus* 4M transfer with each individual IgA$^{high}$ strain having a distinct relative abundance (Fig. 4e). Finally, we replicated these results in mice pre-colonized with another IgA$^{low}$ *B. ovatus* strain *R* (Supplementary Fig. 7c,d).

To validate these results in the setting of more complex gut microbiotas, we performed similar experiments using either gnotobiotic mice colonized by a synthetic cocktail of diverse bacterial species that included *B. ovatus* IgA$^{low}$ strain *Q* (Supplementary Table 5) or gnotobiotic

mice colonized with arrayed culture collections established from donors harboring a functionally validated IgA$^{low}$ *B. ovatus* strain (Fig. 1h and Supplementary Table 6). As with simpler communities, transfer of the high-IgA phenotype was robustly achieved with *B. ovatus* 4M or a multiplex cocktail of eight IgA$^{high}$ *B. ovatus* strains (*B. ovatus* 8M) (Supplementary Table 4) but not by individual IgA$^{high}$ *B. ovatus* strains (Fig. 4f and Supplementary Fig. 7e). Consistent with our previous findings, IgA was elevated only in the large intestine (Fig. 4g and Supplementary Fig. 7f). The relative proportions of each IgA$^{high}$ strain and total relative abundance of all IgA$^{high}$ strains in the stool of multiplex bacterial cocktail recipient mice varied across recipient microbiota communities (Fig. 4h,i and Supplementary Fig. 7g,h).

To further validate the IgA-inducing properties of our multiplex IgA$^{high}$ *B. ovatus* cocktails, we tested these cocktails in two additional gnotobiotic mouse models colonized by human microbiota arrayed culture collections with low-IgA potential (Supplementary Table 6). Again, we found that the multiplex IgA$^{high}$ *B. ovatus* cocktails robustly increased fecal IgA (Supplementary Fig. 8a-f). Across all of the tested *B. ovatus* 4M and *B. ovatus* 8M recipients, we did not find a correlation between the total relative abundance of IgA$^{high}$ strains and the fecal IgA levels, which indicates that maximizing the total abundance of IgA$^{high}$ *B. ovatus* strains does not necessarily increase gut IgA production (Supplementary Fig 8g-i). In summary, our results demonstrate that transfer of multiplex IgA$^{high}$ *B. ovatus* strain cocktails, but not that of individual IgA$^{high}$ strains, consistently and robustly modulates the immune system (e.g. IgA phenotype) across several complex pre-existing gut microbiota.

## Discussion

Functional differences of pathogenic bacteria at the strain level have been intensively studied in the past decades and are a fundamental component of infectious disease clinical practice. More recently the functional impact of bacterial strain variation is becoming apparent in the context of the protective or disease-enhancing properties of the commensal microbiota[11,12,32,55,56]. Here, we identified that approximately half of the isolated strains from *B. ovatus* species, which is one of the most common species of our gut commensal microbiota, drive increased IgA production in the distal intestinal tract. Interestingly, we did not find that the variation in fecal IgA induced by different *B. ovatus* strains was related to unique genetic lineages amongst strains or the density of the bacteria in the feces. Through manipulation of the pre-existing gut microbiota composition, we discovered that cocktails of IgA$^{high}$ *B. ovatus* strains were more efficient than individual IgA$^{high}$ *B. ovatus* strains in converting mice with low gut IgA production into mice producing large amounts of gut IgA.

IgA$^{high}$ *B. ovatus* strains increased IgA production in distal but not proximal intestinal segments by enhancing the ratio of IgA-secreting B cells. Remarkably, this induction was not dominated by the migration of IgA$^{+}$ B cells from canonical IgA inductive sites, as gnotobiotic mice colonized with either IgA$^{high}$ or IgA$^{low}$ *B. ovatus* strains showed comparable IgA$^{+}$ B cells in PPs and MLNs. One possibility is that IgA$^{high}$ *B. ovatus* strains locally elicit IgA production in the large intestine including cecal patches, ILFs and LP[2,54,57]. Interestingly, mice harboring specific *B. ovatus* strains showed no significant differences in the intestinal abundance of *B. ovatus*, which further highlights the unique IgA-inducing properties of individual strains.

After IgA$^{high}$ *B. ovatus* strain colonization, CD4$^{+}$ T cell-depleted mice showed a reduced ratio of IgA$^{+}$ B cells in the gut, in turn leading to decreased luminal IgA along the entire intestinal tract. Of note, both CD4$^{+}$ T cell-sufficient and T cell-depleted mice produced comparable level of gut IgA at the beginning post colonization, which suggests CD4$^{+}$ T cells play less of a role during the very early stage of IgA induction likely due to the dominance of the TI B cell-

318 activation pathway. Interestingly, a protein from the gut commensal *Lactobacillus rhamnosus*
319 was recently shown to locally elicit IgA production via gut epithelial cells[58]. Thus, further studies
320 will be needed to delineate the precise mechanisms whereby IgA$^{high}$ *B. ovatus* strain colonized
321 mice generate gut IgA. Nevertheless, our study highlights the important contribution of T cells in
322 bacteria-mediated IgA production, especially in the large intestine[59,60].

323 FMT-based manipulation of the gut microbiota has a high success rate in the treatment of
324 recurrent *C. difficile* infection[61]. However, its success in other indications, such as ulcerative
325 colitis, is more limited[62,63]. Although improving bacteria engraftment remains a key therapeutic
326 goal of microbiota manipulation[62-64], identifying new strategies that optimize the transfer of a
327 specific immune phenotype constitutes a therapeutic goal with a potentially larger range of
328 applications. Using IgA induction as an example of immunomodulatory phenotype transfer, our
329 data showed that multiplex bacterial cocktails of IgA$^{high}$ *B. ovatus* strains elicited a more robust
330 phenotype transfer than any individual strain, even in mice with complex gut ecosystem. This
331 multiplex effector strain cocktail strategy was robust across multiple recipients, who had low-IgA
332 phenotype and pre-colonized with different microbiotas, and could represent an effective
333 approach to therapeutically modify gut immune parameters in addition to IgA. Of note, across
334 the tested inductions of IgA via gut microbiota manipulation with IgA$^{high}$ *B. ovatus* strains, we
335 found that no single strain consistently dominated over the others. Thus, multiplex bacterial
336 cocktails do not appear to have “super strains” with dominant IgA-inducing function. Rather, the
337 combination of multiple IgA$^{high}$ effector strains in these cocktails has an IgA-inducing potential
338 superior to that of any individual strain. Intriguingly, the relative abundance of total *B. ovatus*
339 species remained largely stable even after the introduction of one to eight new strains
340 suggesting that these new strains largely share the same ecological niches as that occupied by
341 the pre-existing *B. ovatus*.

342 In summary, our results highlight the importance of bacterial strain variation on the IgA-
343 inducing potential of the gut microbiota. In addition, we also identify a new strategy (e.g.

344 multiplex bacterial strain cocktail) for the exploitation of strain variation in the development of

345 robust microbiota-based immunomodulation therapeutic strategies.

346

## Methods

### Mice

Germ-free C57BL/6 and Swiss Webster mice were bred and maintained in flexible film gnotobiotic isolators (Class Biologically Clean, Ltd.). All mice were group housed with a 12-hour light/dark cycle and allowed *ad libitum* access to diet and water. All animal studies were carried out in accordance with protocols approved by the Institutional Animal Care and Use Committee (IACUC) in Icahn School of Medicine at Mount Sinai.

### Colonization of germ-free mice with cultured bacteria

Germ-free mice (~8 weeks old) were colonized 200-µl aliquot of bacteria suspension via oral gavage. Colonized mice were housed in flexible film vinyl isolators or in filter top cages using previously described techniques[43].

### Growth and isolation of bacterial strains

All bacterial strains were obtained from previously banked stool, public culture repositories or human gut microbiota arrayed culture collections[27]. All bacterial strains isolated for this study were isolated from deidentified stool samples from individuals under a Mount Sinai IRB approved protocol (IRB-16-00008). All bacteria apart from *E. coli* were grown under anaerobic condition at 37°C in Brain Heart Infusion (BHI) medium supplemented with 0.5% yeast extract (Difco Laboratories), 0.4% monosaccharide mixture, 0.3% disaccharide mixture, L-cysteine (0.5 mg/ml; Sigma-Aldrich), malic acid (1 mg/ml; Sigma-Aldrich) and 5 µg/ml hemin. *E. coli* was cultured in LB Broth Miller (EMD Chemicals, Inc.) under aerobic condition at 37°C.

### Quantification of immunoglobulins by ELISA

Total fecal and serum IgA were measured by sandwich ELISA. For total IgA detection, ELISA plates (Corning 3690) were coated with 1 µg/ml goat anti-mouse IgA (SouthernBiotech, AL)

capture antibody overnight at 4°C. Plates were washed and blocked with 1% BSA in PBS for 2 h at room temperature. Diluted samples and standards were added and incubated overnight at 4°C. Captured IgA was detected by horseradish peroxidase (HRP)-conjugated goat anti-mouse IgA antibody (Sigma-Aldrich). ELISA plates were developed by TMB microwell peroxidase substrate (KPL, Inc.) and quenched by 1 M $H_2SO_4$. Colorimetric reaction was measured at OD = 450 nm by a Synergy™ HTX Multi-Mode Microplate Reader (BioTek Instruments, Inc.). Other serum immunoglobulins (IgG1, IgG2a, IgG2b, IgG3, IgM and IgE) were also detected using sandwich ELISA with the following capture and detection antibody pairs (all the following antibodies were purchased from SouthernBiotech, AL): goat anti-mouse IgG1, goat anti-mouse IgG2a, goat anti-mouse IgG2b, goat anti-mouse IgG3, rat anti-mouse IgE, rat anti-mouse IgM, goat anti-mouse IgG-HRP, goat anti-mouse IgE-HRP and goat anti-mouse IgM-HRP. Corresponding mouse immunoglobulin isotypes were used as standards.

**Depletion of $CD4^+$ T Cells in germ-free mice**

*In vivo* depletion of $CD4^+$ T cells was performed as described[65]. Briefly, gnotobiotic mice (8 weeks old) were first injected intraperitoneally (i.p.) with anti-mouse CD4 monoclonal antibody (Bio X Cell, clone GK1.5) or matched isotype control (Bio X Cell, clone LTF-2) at 0.5 mg/day/mouse for 3 consecutive days. Then the injection was performed every 3 days for a period of 3 weeks. Five days after the first antibody injection, mice were inoculated via oral gavage with *B. ovatus* strain *E*. Efficacy of T cell depletion was evaluated by flow cytometry.

**Lymphocyte isolation from tissues**

To isolate mononuclear cells from Peyer's patches (PPs), PPs were excised from mouse small intestines and incubated in dissociation buffer, containing Hank's Balanced Salt Solution (HBSS) without $Ca^{2+}$ and $Mg^{2+}$ (GIBCO), 10% fetal bovine serum (FBS), 5 mM EDTA and 15 mM HEPES, at 37°C for 30 min. Later, tissues were mechanically separated by pushing them

399 through a 70 μm strainer into Iscove's Modified Dulbecco's Medium (IMDM) supplemented with
400 2% FBS. Filtered cells were spun down, washed and resuspended in IMDM/2%FBS. Lamina
401 propria lymphocytes were isolated as described[27]. Briefly, small intestines and colons were
402 excised, followed by removing visceral fat and intestinal contents. Tissues were opened
403 longitudinally, washed twice in HBSS and incubated in dissociation buffer for 30 min at 37°C
404 with mild agitation to remove epithelium and intraepithelial lymphocytes. Tissues were then
405 washed three times in ice cold HBSS, cut into ~2 cm pieces and digested with collagenase
406 (Sigma-Aldrich), DNase I (Sigma-Aldrich) and dispase I (Corning). Cell suspensions were
407 filtered through 70 μm cell strainers, washed three times, and resuspended in IMDM/2%FBS.
408 Mesenteric lymph nodes were separated from mesenteric fat and dissociated in IMDM/2%FBS
409 by physically pressing the tissues between the frosted portions of two glass microscope slides.
410 The cell suspension was filtered through a 70 μm cell strainer, washed three times and
411 resuspended in IMDM/2%FBS
412
413 **Detection of IgA-coated bacteria in feces**
414 IgA-coated fecal bacteria were measured by flow cytometry as previously described[12,13]. Briefly,
415 mouse fecal pellets, stored at -80°C freezer after collection, were dissolved in PBS to a final
416 concentration of 100 milligram per milliliter PBS by weight, thawed at room temperature,
417 homogenized in vortex mixer and centrifuged at 4°C to remove large particles. The supernatant
418 was passed through a 40 μm sterile nylon filter and 50 μl aliquot of the bacteria suspension was
419 collected for staining. Bacteria were pelleted by centrifugation and washed in 1ml of
420 PBS/1%BSA/2mM EDTA for 3 times. Non-specific binding sites were first blocked with 50 μl
421 PBS/1%BSA/20% rat serum for 20 min at 4°C. Bacteria were then stained with 50 μl
422 of PBS/1%BSA/2mM EDTA buffer containing 1:100 dilution of monoclonal rat anti-mouse IgA
423 antibody (eBioscience, clone mA-6E1) for 30 min at 4°C. After washing 3 times, bacterial pellets
424 were resuspended in PBS containing SYBR Green I (1:100,000 dilution; Invitrogen). Samples

were run through a BD LSR Fortessa™ cell analyzer and further analyzed by FlowJo software (Tree Star, Inc.). Only SYBR positive events were regarded as bacteria and gated for further quantification of IgA-coated bacteria (Supplementary Fig. 9).

**Flow cytometry analysis and antibodies**

Isolated mononuclear cells were washed in PBS and incubated with Zombie Aqua™ dye (BioLegend) to distinguish live and dead cells. Before surface staining, non-specific binding of immunoglobulin to Fc receptors was blocked by anti-mouse CD16/32 antibody (BD Biosciences). Cells were stained in FACS buffer (PBS without $Ca^{2+}$/$Mg^{2+}$ supplemented with 2% FBS and 2 mM EDTA) containing a mix of antibodies for 30 min at 4°C. The following antibodies were purchased from BioLegend if not indicated otherwise: anti-mouse CD45 (clone 30-F11), anti-mouse/human CD45R/B220 (clone RA3-6B2), anti-mouse GL7 (clone GL7), anti-mouse CD4 (clone GK1.5), anti-mouse IgA (eBioscience, clone mA-6E1). For the staining of $IgA^+$ cells, both surface and intracellular staining were performed. Multi-parameter analysis was conducted with BD™ LSR II flow cytometry and analyzed with FlowJo software (Tree Star, Inc.). Only live cells and singlets were used in all analyses (Supplementary Fig. 9).

**Extraction of bacterial DNA from feces**

Each murine fecal pellet was collected into a 2 ml screw cap tube (Axygen Scientific, SCT200SSC) and stored at -80°C freezer until processing. Each sample was mixed with 1.3 ml of buffer, composed of 282 µl of DNA buffer A (20 mM Tris pH 8.0, 2 mM EDTA and 200 mM NaCl), 200 µl of 20% SDS (v/w), 550 µl of Phenol:Chloroform:IAA (25:24:1) (Ambion, AM9732) and 268 µl of Buffer PM (Qiagen, 19083), and 400 µl of 0.1 mm diameter zirconia/silica beads (BioSpec, 11079101z). Next, the sample was mechanically lysed with a Mini-Beadbeater-96 (BioSpec, 1001) for 5 min at room temperature. After centrifuging for 5 min at 4000 rpm (Eppendorf Centrifuge 5810 R), all aqueous phase was collected, mixed with 650 µl of Buffer

PM thoroughly before running through a Qiagen spin column. The column was washed twice with Buffer PE (Qiagen, 19065). Attached DNA was eluted with 100 µl of Buffer EB (Qiagen, 19086) and quantified with Qubit™ dsDNA Assay Kit (Thermo Fisher Scientific, Q32853/Q32854). Bacteria density was calculated by the following equation: Bacteria Density = DNA yield per sample (ug) / weight of sample (mg)[66].

**Bacterial genome and metagenomic sequencing**

Purified bacterial template DNA (~250 ng) was sonicated and prepared using the NEBNext® Ultra™ II DNA Library Prep kit. Samples were pooled and sequenced with an Illumina HiSeq 4000 with pair-end 150nt reads. Metagenomic sequencing reads were mapped back to the reference genomes for each experiment to determine the relative abundance of each strain. To uniquely distinguish each strain, 100K sequencing reads for each sample were mapped to the unique regions of each genome and final abundances were scaled by the unique genome size of each strain (i.e. genome equivalents), as previously described[67].

**Immunofluorescence staining**

Immunofluorescence staining was performed as described previously[25,60]. Briefly, intestinal tissues were fixed in 10% neutral formalin overnight at 4°C, dehydrated in 15% and 30% sucrose buffer sequentially and mounted in O.C.T Embedding Compound (Electron Microscopy Sciences). Cryostat sections (~8 µm) were prepared, blocked with anti-CD16/32 antibody in 10% (v/v) rat serum/0.1% Triton-X100 in PBS for 30 min at room temperature and incubated with the indicated primary antibodies at 4°C overnight. The following primary antibodies were used: rat anti-mouse IgA-FITC (1/300 dilution; eBioscience, clone mA-6E1), goat anti-mouse pIgR (1/500 dilution; R&D Systems, cat #: AF2800). Slides were washed in PBS for three times, incubated with Alexa Fluor®-conjugated species-specific secondary antibody (1/400 dilution; Invitrogen) for 1 h at room temperature if needed and finally mounted with ProLong® Gold Anti-

fade Reagent with DAPI (Invitrogen). Fluorescence images of sections were acquired with a LSM780 confocal laser-scanning microscope (Carl Zeiss) and further processed in ImageJ if necessary.

**Statistical analysis**

Data are shown as mean ± SEM. Statistical significance between two groups was assessed by an unpaired, two-tailed Student's *t* test. Comparisons among three or more groups were performed using One-way ANOVA. Bimodality distribution of IgA levels induced by different *B. ovatus* strains was performed in R (R package 'diptest'). For correlation test, Pearson correlation coefficient was employed. Data plotting, interpolation and statistical analysis were performed using GraphPad Prism 6.0 (GraphPad Software, La Jolla, CA) or R statistical software (version 3.2.2). A *p*-value less than 0.05 is considered statistically significant.

## Data availability

Bacterial genomes and metagenomic sequencing reads for this study are available via NCBI BioProject accession number PRJNA518912.

## Acknowledgments

We are grateful to C. Fermin, E. Vazquez, and G. Escano for the husbandry of gnotobiotic mice; Drs. Anuk Das, Dirk Gevers, C. Cunningham-Rundles, B. Brown and T. Moran for helpful discussions and comments. This work was supported in part by the staff and resources of the Gnotobiotic Mouse Core Facility, the Microbiome Translational Center, the Flow Cytometry Core Facility and the Scientific Computing Division in Icahn School of Medicine at Mount Sinai. This work was supported by National Institutes of Health Grants (NIGMS GM108505 and NCCIH AT008661) and Janssen Human Microbiome Institute (to J.J.F.) and NIH DK112679 (to E.J.C.).

## Author contributions

C.Y. and J.J.F conceived the study and designed the experiments; C.Y., I.M., E.J.C., J.B., V.A., E.G., D.H., M.D. and J.J.F. collected samples and conducted the experiments; I.M. and Z.L. provided bacterial isolates; C.Y., S.M., A.C. and J.J.F. analyzed data; C.Y. and J.J.F. prepared the manuscript. All authors read and approved the final manuscript.

## Competing interests

J.J.F. serves as a consultant for Janssen Research & Development LLC. The other authors declare no conflict of interests.

## References


1 Sutherland, D. B., Suzuki, K. & Fagarasan, S. Fostering of advanced mutualism with gut microbiota by Immunoglobulin A. *Immunological Reviews* **270**, 20-31, doi:10.1111/imr.12384 (2016).

2 Cerutti, A. & Rescigno, M. The biology of intestinal immunoglobulin A responses. *Immunity* **28**, 740-750, doi:10.1016/j.immuni.2008.05.001 (2008).

3 Macpherson, A. J., Geuking, M. B. & McCoy, K. D. Homeland Security: IgA immunity at the frontiers of the body. *Trends Immunol* **33**, 160-167, doi:10.1016/j.it.2012.02.002 (2012).

4 Okai, S. *et al.* High-affinity monoclonal IgA regulates gut microbiota and prevents colitis in mice. *Nat Microbiol* **1**, 16103, doi:10.1038/nmicrobiol.2016.103 (2016).

5 Tokuhara, D. *et al.* Secretory IgA-mediated protection against V. cholerae and heat-labile enterotoxin-producing enterotoxigenic Escherichia coli by rice-based vaccine. *Proc Natl Acad Sci U S A* **107**, 8794-8799, doi:10.1073/pnas.0914121107 (2010).

6 Strugnell, R. A. & Wijburg, O. L. C. The role of secretory antibodies in infection immunity. *Nat Rev Microbiol* **8**, 656-667, doi:10.1038/nrmicro2384 (2010).

7 Fagarasan, S. Evolution, development, mechanism and function of IgA in the gut. *Curr Opin Immunol* **20**, 170-177, doi:10.1016/j.coi.2008.04.002 (2008).

8 Pabst, O. New concepts in the generation and functions of IgA. *Nature Reviews Immunology* **12**, 821-832, doi:10.1038/nri3322 (2012).

9 McLoughlin, K., Schluter, J., Rakoff-Nahoum, S., Smith, A. L. & Foster, K. R. Host Selection of Microbiota via Differential Adhesion. *Cell Host Microbe* **19**, 550-559, doi:10.1016/j.chom.2016.02.021 (2016).

10 Donaldson, G. P. *et al.* Gut microbiota utilize immunoglobulin A for mucosal colonization. *Science* **360**, 795-800, doi:10.1126/science.aaq0926 (2018).

11 Viladomiu, M. *et al.* IgA-coated E. coli enriched in Crohn's disease spondyloarthritis promote TH17-dependent inflammation. *Sci Transl Med* **9**, doi:10.1126/scitranslmed.aaf9655 (2017).

12 Palm, N. W. *et al.* Immunoglobulin A coating identifies colitogenic bacteria in inflammatory bowel disease. *Cell* **158**, 1000-1010, doi:10.1016/j.cell.2014.08.006 (2014).

13 Kau, A. L. *et al.* Functional characterization of IgA-targeted bacterial taxa from undernourished Malawian children that produce diet-dependent enteropathy. *Sci Transl Med* **7**, 276ra224, doi:10.1126/scitranslmed.aaa4877 (2015).

14 Macpherson, A. J. *et al.* A primitive T cell-independent mechanism of intestinal mucosal IgA responses to commensal bacteria. *Science* **288**, 2222-+, doi:DOI 10.1126/science.288.5474.2222 (2000).

15 Hapfelmeier, S. *et al.* Reversible microbial colonization of germ-free mice reveals the dynamics of IgA immune responses. *Science* **328**, 1705-1709, doi:10.1126/science.1188454 (2010).

16 Peterson, D. A., McNulty, N. P., Guruge, J. L. & Gordon, J. I. IgA response to symbiotic bacteria as a mediator of gut homeostasis. *Cell Host Microbe* **2**, 328-339, doi:10.1016/j.chom.2007.09.013 (2007).

17 Fritz, J. H. *et al.* Acquisition of a multifunctional IgA+ plasma cell phenotype in the gut. *Nature* **481**, 199-203, doi:10.1038/nature10698 (2011).

18 Macpherson, A. J., McCoy, K. D., Johansen, F. E. & Brandtzaeg, P. The immune geography of IgA induction and function. *Mucosal Immunol* **1**, 11-22, doi:10.1038/mi.2007.6 (2008).

19 Bunker, J. J. *et al.* Innate and Adaptive Humoral Responses Coat Distinct Commensal Bacteria with Immunoglobulin A. *Immunity* **43**, 541-553, doi:10.1016/j.immuni.2015.08.007 (2015).

20 Lindner, C. *et al.* Diversification of memory B cells drives the continuous adaptation of secretory antibodies to gut microbiota. *Nat Immunol* **16**, 880-888, doi:10.1038/ni.3213 (2015).

21 Obata, T. *et al.* Indigenous opportunistic bacteria inhabit mammalian gut-associated lymphoid tissues and share a mucosal antibody-mediated symbiosis. *P Natl Acad Sci USA* **107**, 7419-7424, doi:10.1073/pnas.1001061107 (2010).

22 Lecuyer, E. *et al.* Segmented filamentous bacterium uses secondary and tertiary lymphoid tissues to induce gut IgA and specific T helper 17 cell responses. *Immunity* **40**, 608-620, doi:10.1016/j.immuni.2014.03.009 (2014).

23 Chudnovskiy, A. *et al.* Host-Protozoan Interactions Protect from Mucosal Infections through Activation of the Inflammasome. *Cell* **167**, 444-456 e414, doi:10.1016/j.cell.2016.08.076 (2016).

24 Shibata, N. *et al.* Lymphoid tissue-resident Alcaligenes LPS induces IgA production without excessive inflammatory responses via weak TLR4 agonist activity. *Mucosal Immunol*, doi:10.1038/mi.2017.103 (2018).

25 Moon, C. *et al.* Vertically transmitted faecal IgA levels determine extra-chromosomal phenotypic variation. *Nature* **521**, 90-93, doi:10.1038/nature14139 (2015).

26 Macpherson, A. J., Koller, Y. & McCoy, K. D. The bilateral responsiveness between intestinal microbes and IgA. *Trends Immunol* **36**, 460-470, doi:10.1016/j.it.2015.06.006 (2015).

27 Faith, J. J., Ahern, P. P., Ridaura, V. K., Cheng, J. & Gordon, J. I. Identifying gut microbe-host phenotype relationships using combinatorial communities in gnotobiotic mice. *Sci Transl Med* **6**, 220ra211, doi:10.1126/scitranslmed.3008051 (2014).

28 Atarashi, K. *et al.* Induction of colonic regulatory T cells by indigenous Clostridium species. *Science* **331**, 337-341, doi:10.1126/science.1198469 (2011).

29 Round, J. L. & Mazmanian, S. K. Inducible Foxp3+ regulatory T-cell development by a commensal bacterium of the intestinal microbiota. *Proc Natl Acad Sci U S A* **107**, 12204-12209, doi:10.1073/pnas.0909122107 (2010).

30 Ivanov, II *et al.* Induction of intestinal Th17 cells by segmented filamentous bacteria. *Cell* **139**, 485-498, doi:10.1016/j.cell.2009.09.033 (2009).

31 Mortha, A. *et al.* Microbiota-dependent crosstalk between macrophages and ILC3 promotes intestinal homeostasis. *Science* **343**, 1249288, doi:10.1126/science.1249288 (2014).

32 Britton, G. J. *et al.* Microbiotas from Humans with Inflammatory Bowel Disease Alter the Balance of Gut Th17 and RORgammat(+) Regulatory T Cells and Exacerbate Colitis in Mice. *Immunity* **50**, 212-224 e214, doi:10.1016/j.immuni.2018.12.015 (2019).

33 Clemente, J. C., Manasson, J. & Scher, J. U. The role of the gut microbiome in systemic inflammatory disease. *BMJ* **360**, j5145, doi:10.1136/bmj.j5145 (2018).

34 Smillie, C. S. *et al.* Strain Tracking Reveals the Determinants of Bacterial Engraftment in the Human Gut Following Fecal Microbiota Transplantation. *Cell Host Microbe* **23**, 229-240 e225, doi:10.1016/j.chom.2018.01.003 (2018).

35 Seekatz, A. M. *et al.* Recovery of the gut microbiome following fecal microbiota transplantation. *MBio* **5**, e00893-00814, doi:10.1128/mBio.00893-14 (2014).

36 Shankar, V. *et al.* Species and genus level resolution analysis of gut microbiota in Clostridium difficile patients following fecal microbiota transplantation. *Microbiome* **2**, 13, doi:10.1186/2049-2618-2-13 (2014).

37 Clemente, J. C. & Dominguez-Bello, M. G. Safety of vaginal microbial transfer in infants delivered by caesarean, and expected health outcomes. *BMJ* **352**, i1707, doi:10.1136/bmj.i1707 (2016).

38 Petrof, E. O. & Khoruts, A. From stool transplants to next-generation microbiota therapeutics. *Gastroenterology* **146**, 1573-1582, doi:10.1053/j.gastro.2014.01.004 (2014).
39 Human Microbiome Project, C. Structure, function and diversity of the healthy human microbiome. *Nature* **486**, 207-214, doi:10.1038/nature11234 (2012).
40 Turnbaugh, P. J. *et al.* A core gut microbiome in obese and lean twins. *Nature* **457**, 480-484, doi:10.1038/nature07540 (2009).
41 Kanasugi, H. *et al.* Single administration of enterococcal preparation (FK-23) augments non-specific immune responses in healthy dogs. *Int J Immunopharmacol* **19**, 655-659 (1997).
42 Reber, S. O. *et al.* Immunization with a heat-killed preparation of the environmental bacterium Mycobacterium vaccae promotes stress resilience in mice. *Proc Natl Acad Sci U S A* **113**, E3130-3139, doi:10.1073/pnas.1600324113 (2016).
43 Faith, J. J. *et al.* The long-term stability of the human gut microbiota. *Science* **341**, 1237439, doi:10.1126/science.1237439 (2013).
44 Faith, J. J., Colombel, J.-F. & Gordon, J. I. Identifying strains that contribute to complex diseases through the study of microbial inheritance. *Proceedings of the National Academy of Sciences* **112**, 633-640, doi:10.1073/pnas.1418781112 (2015).
45 Shijie Zhao, T. D. L., Mathilde poyet, Sean M. Gibbons, Mathieu Groussin, Ramnik J. Xavier, Eric J. Alm. Adaptive evolution within the gut microbiome of individual people. *BioRxiv*, doi:https://doi.org/10.1101/208009 (2018).
46 Vatanen, T. *et al.* Genomic variation and strain-specific functional adaptation in the human gut microbiome during early life. *Nat Microbiol*, doi:10.1038/s41564-018-0321-5 (2018).
47 Kim, M., Qie, Y., Park, J. & Kim, C. H. Gut Microbial Metabolites Fuel Host Antibody Responses. *Cell Host Microbe* **20**, 202-214, doi:10.1016/j.chom.2016.07.001 (2016).
48 Fransen, F. *et al.* BALB/c and C57BL/6 Mice Differ in Polyreactive IgA Abundance, which Impacts the Generation of Antigen-Specific IgA and Microbiota Diversity. *Immunity* **43**, 527-540, doi:10.1016/j.immuni.2015.08.011 (2015).
49 Johansen, F. E. & Kaetzel, C. S. Regulation of the polymeric immunoglobulin receptor and IgA transport: new advances in environmental factors that stimulate pIgR expression and its role in mucosal immunity. *Mucosal Immunol* **4**, 598-602, doi:10.1038/mi.2011.37 (2011).
50 Hooper, L. V. *et al.* Molecular analysis of commensal host-microbial relationships in the intestine. *Science* **291**, 881-884, doi:10.1126/science.291.5505.881 (2001).
51 Schneeman, T. A. *et al.* Regulation of the Polymeric Ig Receptor by Signaling through TLRs 3 and 4: Linking Innate and Adaptive Immune Responses. *The Journal of Immunology* **175**, 376-384, doi:10.4049/jimmunol.175.1.376 (2005).
52 Chorny, A., Puga, I. & Cerutti, A. Innate Signaling Networks in Mucosal IgA Class Switching. *Adv Immunol* **107**, 31-69, doi:10.1016/S0065-2776(10)07006-9 (2010).
53 Suzuki, K., Kawamoto, S., Maruya, M. & Fagarasan, S. GALT: Organization and Dynamics Leading to IgA Synthesis. *Adv Immunol* **107**, 153-185, doi:10.1016/S0065-277600)07003-3 (2010).
54 Fagarasan, S., Kawamoto, S., Kanagawa, O. & Suzuki, K. Adaptive immune regulation in the gut: T cell-dependent and T cell-independent IgA synthesis. *Annu Rev Immunol* **28**, 243-273, doi:10.1146/annurev-immunol-030409-101314 (2010).
55 Palmela, C. *et al.* Adherent-invasive Escherichia coli in inflammatory bowel disease. *Gut* **67**, 574-587, doi:10.1136/gutjnl-2017-314903 (2018).
56 Arthur, J. C. *et al.* Intestinal inflammation targets cancer-inducing activity of the microbiota. *Science* **338**, 120-123, doi:10.1126/science.1224820 (2012).

57 Masahata, K. *et al.* Generation of colonic IgA-secreting cells in the caecal patch. *Nat Commun* **5**, 3704, doi:10.1038/ncomms4704 (2014).
58 Wang, Y. *et al.* An LGG-derived protein promotes IgA production through upregulation of APRIL expression in intestinal epithelial cells. *Mucosal Immunol* **10**, 373-384, doi:10.1038/mi.2016.57 (2017).
59 Kawamoto, S. *et al.* Foxp3(+) T cells regulate immunoglobulin a selection and facilitate diversification of bacterial species responsible for immune homeostasis. *Immunity* **41**, 152-165, doi:10.1016/j.immuni.2014.05.016 (2014).
60 Kunisawa, J. *et al.* Microbe-dependent CD11b+ IgA+ plasma cells mediate robust early-phase intestinal IgA responses in mice. *Nat Commun* **4**, 1772, doi:10.1038/ncomms2718 (2013).
61 van Nood, E. *et al.* Duodenal infusion of donor feces for recurrent Clostridium difficile. *N Engl J Med* **368**, 407-415, doi:10.1056/NEJMoa1205037 (2013).
62 Moayyedi, P. *et al.* Fecal Microbiota Transplantation Induces Remission in Patients With Active Ulcerative Colitis in a Randomized Controlled Trial. *Gastroenterology* **149**, 102-+, doi:10.1053/j.gastro.2015.04.001 (2015).
63 Rossen, N. G. *et al.* Findings From a Randomized Controlled Trial of Fecal Transplantation for Patients With Ulcerative Colitis. *Gastroenterology* **149**, 110-118 e114, doi:10.1053/j.gastro.2015.03.045 (2015).
64 Grinspan, A. M. & Kelly, C. R. Fecal Microbiota Transplantation for Ulcerative Colitis: Not Just Yet. *Gastroenterology* **149**, 15-18, doi:10.1053/j.gastro.2015.05.030 (2015).
65 Kruisbeek, A. M. In vivo depletion of CD4- and CD8-specific T cells. *Curr Protoc Immunol* **Chapter 4**, Unit 4 1, doi:10.1002/0471142735.im0401s01 (2001).
66 Contijoch, E. J. *et al.* Gut microbiota density influences host physiology and is shaped by host and microbial factors. *Elife* **8**, doi:10.7554/eLife.40553 (2019).
67 McNulty, N. P., Wu, M., Erickson, A. R., Pan, C. & Erickson, B. K. Effects of Diet on Resource Utilization by a Model Human Gut Microbiota Containing Bacteroides cellulosilyticus WH2, a Symbiont with an Extensive Glycobiome. *PLoS biology* **11**, e1001637, doi:10.1371/journal.pbio.1001637 (2013).

# Figures

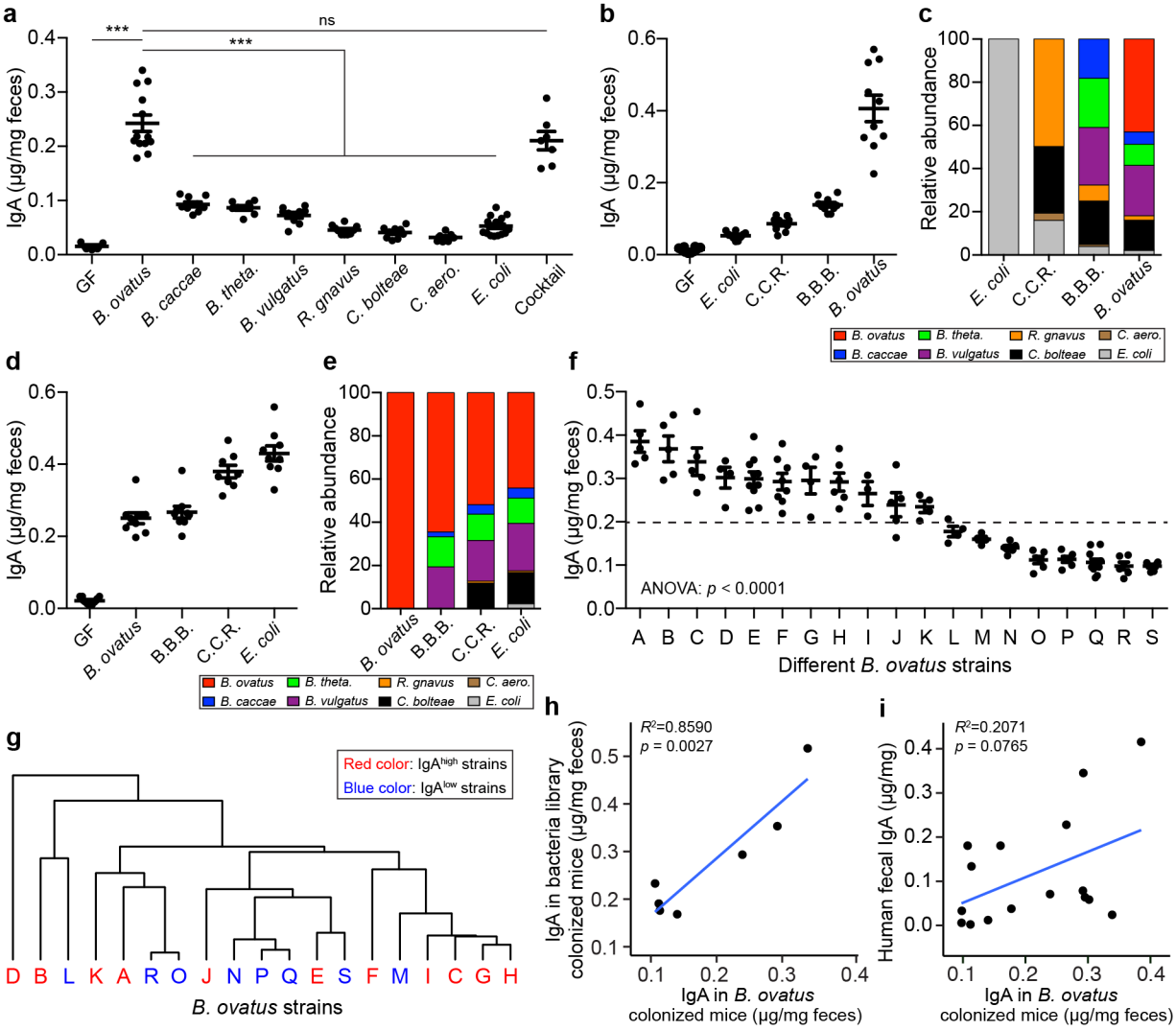


**Fig. 1 | *B. ovatus* species, with strain-level differences, predominantly induces fecal IgA production in gnotobiotic mice.** (**a**) Fecal IgA level in C57BL/6 gnotobiotic mice colonized with individual or a cocktail of human gut commensal bacteria for three weeks. (**b**-**e**) The concentration of fecal IgA (**b** and **d**) and proportion of each bacterial strain (**c** and **e**) in stool of gnotobiotic mice that were colonized sequentially with individual or combined bacterial communities starting from *E. coli* (**b** and **c**) or *B. ovatus* (**d** and **e**). Feces were harvested before addition of new bacteria to the same mice. C.C.R.: cocktail of *C. bolteae, C. aerofaciens* and *R. gnavus*; B.B.B.: cocktail of *B. caccae, B. theta.* and *B. vulgatus* (**f**) Quantification of fecal IgA in

703 gnotobiotic mice upon colonization with an individual strain of *B. ovatus* for three weeks. Unique
704 strains of *B. ovatus* were isolated from the stools of different human donors. Dotted line
705 separates high- and low-IgA phenotypes. (**g**) Dendrogram clustering of different *B. ovatus*
706 strains basing on the dissimilarity of bacterial genomic DNA sequences. (**h**) Correlation of stool
707 IgA levels between single *B. ovatus* strain monocolonized mice versus mice colonized with a
708 microbiota arrayed culture collection that included that single *B. ovatus* strain. Both single *B.*
709 *ovatus* strains and arrayed culture collections were isolated from the same donor. (**i**) Correlation
710 of fecal IgA concentration between single *B. ovatus* strain colonized mice versus human donor.
711 Data shown are mean ± standard error of the mean. Each dot in **a**, **b**, **d** and **f** represents a
712 biological replicate. The average fecal IgA concentration from 4-10 mice was used for
713 correlation in **h** and **i**. Detailed strain information is listed in Supplementary Tables 1 and 2. *p*-
714 values with statistical significance (assessed by two-tailed Student's *t* test or one-way ANOVA)
715 are indicated: ***$p < 0.001$; ns, not significant.
716

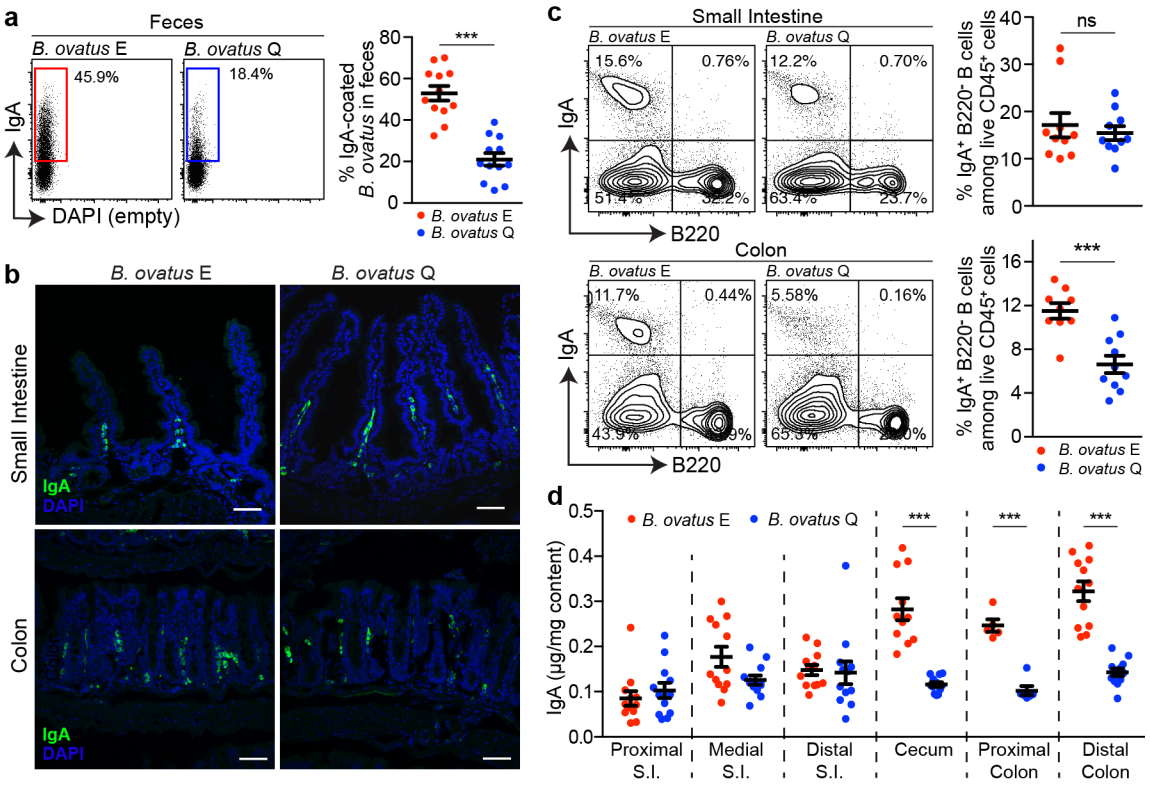


**Fig. 2 | IgA$^{high}$ *B. ovatus* strain elicits stronger IgA responses in the large intestine.** (**a**) Representative flow cytometry plot and quantification of IgA-coated *B. ovatus* in feces of gnotobiotic mice harboring either *B. ovatus* strain *E* or *Q*. (**b**) Representative images of IgA$^+$ cells in small intestine and the colon are shown. IgA$^+$ cells were stained with anti-IgA (green); Nuclei were counter-stained with DAPI (4',6-diamidino-2-phenylindole) (blue). n = 5~6. Scale bar = 50 μm. (**c**) Percentage of IgA$^+$ B cells in small intestinal and colonic tissues is shown. LP lymphocytes were analyzed by flow cytometry. Number adjacent to gate represents percentage. (**d**) Free IgA concentration in luminal contents along the length of the intestine. S.I.: small intestine. Data shown are mean ± standard error of the mean. Each dot represents an individual mouse. *p*-values with statistical significance (assessed by two-tailed Student's *t* test) are indicated: ***$p < 0.001$; ns, not significant.

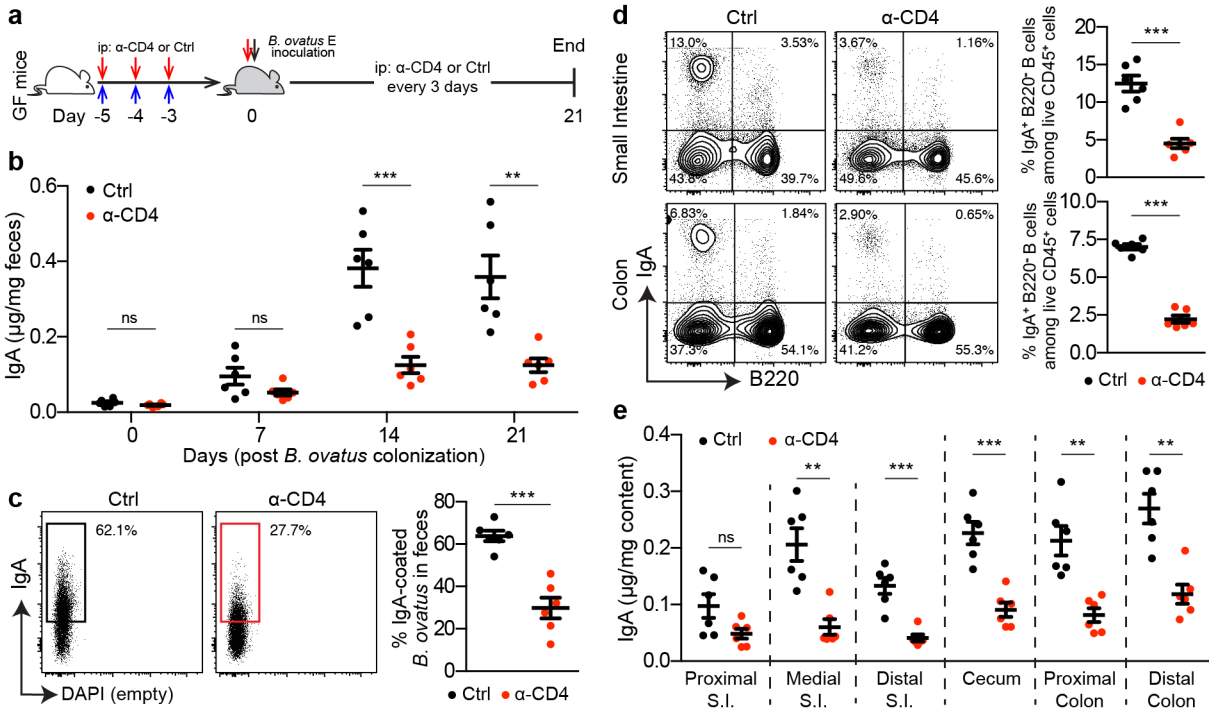


**Fig. 3 | Both T-cell-dependent and T-cell-independent pathways are involved in fecal IgA induction mediated by *B. ovatus* strain *E*.** (**a**) Schematic representation of $CD4^+$ T cells depletion in GF B6 mice is illustrated. Red arrows represent i.p. injection of anti-CD4 antibody or isotype control. Black arrow indicates *B. ovatus* strain *E* inoculation and blue arrows represent time. (**b**) Dynamics of fecal IgA concentration in *B. ovatus* strain *E* inoculated gnotobiotic B6 mice treated with either anti-CD4 antibody or isotype control. (**c**) Representative flow cytometry plot and quantification of IgA-coated bacteria in feces of *B. ovatus* strain-*E*-colonized gnotobiotic mice treated with either anti-CD4 antibody or isotype control. (**d**) Representative flow cytometry plot and percentage of $IgA^+$ B cells in small intestine and the colon are shown. Numbers adjacent to gates represent percentage. (**e**) Concentration of free IgA in the intestinal content collected from different regions of the whole intestinal tract is shown. S.I.: small intestine. Data shown are mean ± standard error of the mean. Each dot represents an individual mouse. *p*-values with statistical significance (assessed by two-tailed Student's *t* test) are indicated: $^{**}p < 0.01$, $^{***}p < 0.001$; ns, not significant.

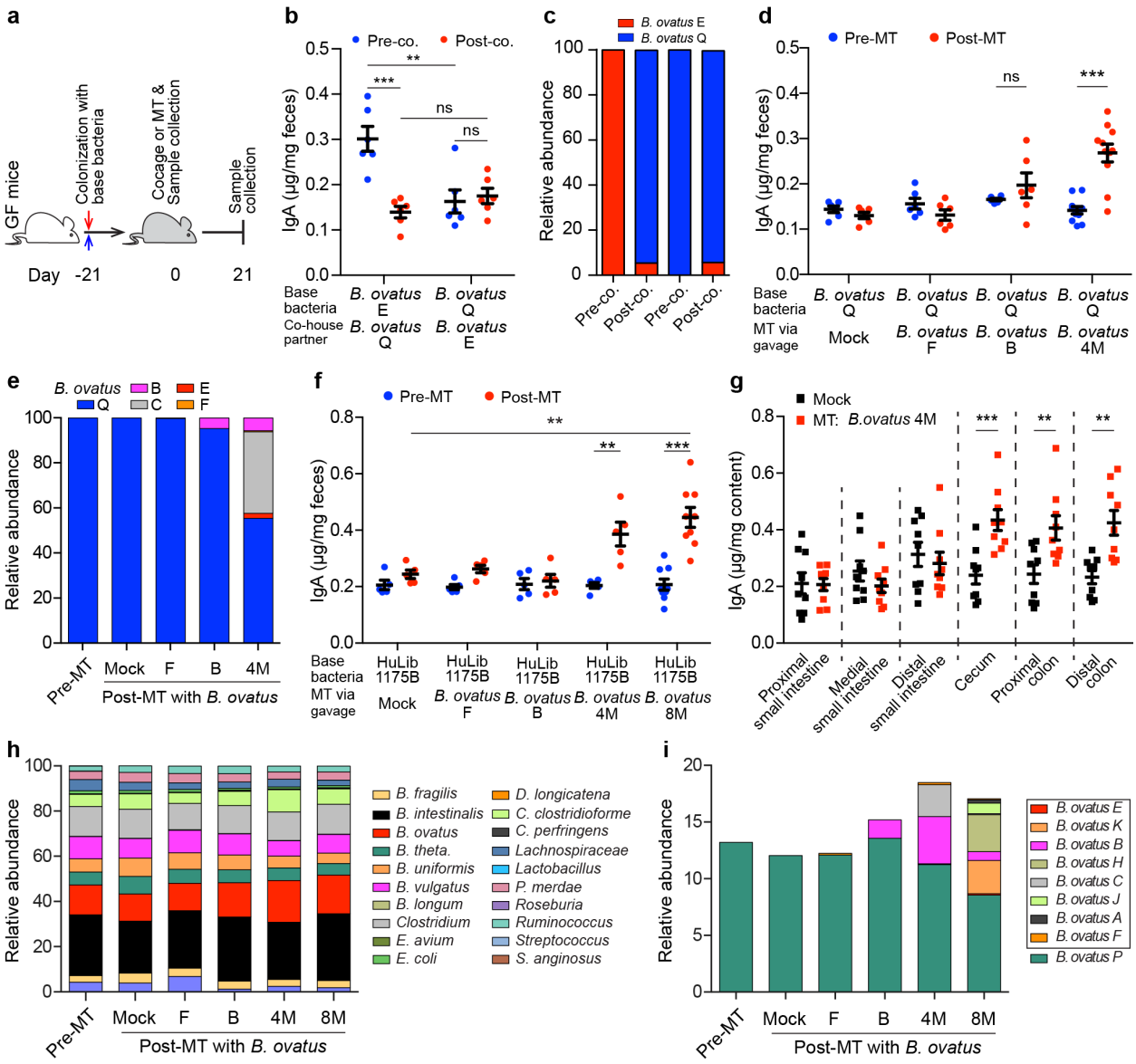


**Fig. 4 | Multiplex microbial strains robustly transfer high-IgA phenotype to low-IgA producing mice.** (**a**) Schematic representation of cohousing and microbial therapeutic strategies. (**b** and **c**) Fecal IgA concentration (**b**) and relative abundance of each *B. ovatus* strain (**c**) in pre- and post-cohoused gnotobiotic mice, which were pre-colonized with either *B. ovatus* strain *E* or *Q*. (**d** and **e**) Fecal IgA concentration (**d**) and relative abundance of each *B. ovatus* strain (**e**) in mice pre- and post-microbiota-based therapeutic (MT). Mice were first colonized with *B. ovatus* strain *Q* for three weeks and subsequently administered a microbial therapeutic comprised of either an individual IgA$^{high}$ *B. ovatus* strain or a cocktail of IgA$^{high}$ *B.*

*ovatus* strains. (**f**) Fecal IgA concentration in mice pre- and post-MT, which were pre-colonized with human microbiota arrayed culture collection (e.g. HuLib1175B) for three weeks. The therapeutic was either an individual IgA$^{high}$ *B. ovatus* strain or a cocktail of IgA$^{high}$ *B. ovatus* strains. *B. ovatus* 4M: a cocktail of 4 different IgA$^{high}$ *B. ovatus* strains; *B. ovatus* 8M: a cocktail of 8 different IgA$^{high}$ *B. ovatus* strains. (**g**) Free IgA concentration along the intestinal tract of mice after gavage with Mock or *B. ovatus* 4M. (**h**) Relative abundance of bacterial species in mice pre- and post-MT. (**i**) Relative abundance of different *B. ovatus* strains in mice pre- and post-MT. Data shown are mean ± standard error of the mean. Sequencing plots display the average abundance from five mice. Each dot represents a biological replicate. Detailed strain information is listed in Supplementary Tables 2 and 6. *p*-values with statistical significance (assessed by two-tailed Student's *t* test) are indicated: $^{**}p < 0.01$, $^{***}p < 0.001$; ns, not significant.